Atmos. Chem. Phys., 15, 6023–6034, 2015
www.atmos-chem-phys.net/15/6023/2015/
doi:10.5194/acp-15-6023-2015

Atmospheric Chemistry and Physics
Open Access

Aerosol composition and sources during the Chinese Spring Festival: fireworks, secondary aerosol, and holiday effects

Q. Jiang[1,3], Y. L. Sun[1,2], Z. Wang[1], and Y. Yin[2,3]

[1]State Key Laboratory of Atmospheric Boundary Layer Physics and Atmospheric Chemistry, Institute of Atmospheric Physics, Chinese Academy of Sciences, Beijing 100029, China
[2]Collaborative Innovation Center on Forecast and Evaluation of Meteorological Disasters, Nanjing University of Information Science & Technology, Nanjing 210044, China
[3]Key Laboratory for Aerosol-Cloud-Precipitation of China Meteorological Administration, Nanjing University of Information Science & Technology, Nanjing 210044, China

Correspondence to: Y. L. Sun (sunyele@mail.iap.ac.cn)

Received: 12 June 2014 – Published in Atmos. Chem. Phys. Discuss.: 11 August 2014
Revised: 16 April 2015 – Accepted: 12 May 2015 – Published: 2 June 2015

Abstract. Aerosol particles were characterized by an Aerodyne aerosol chemical speciation monitor along with various collocated instruments in Beijing, China, to investigate the role of fireworks (FW) and secondary aerosol in particulate pollution during the Chinese Spring Festival of 2013. Three FW events, exerting significant and short-term impacts on fine particles ($PM_{2.5}$), were observed on the days of Lunar New Year, Lunar Fifth Day, and Lantern Festival. The FW were shown to have a large impact on non-refractory potassium, chloride, sulfate, and organics in submicron aerosol (PM_1), of which FW organics appeared to be emitted mainly in secondary, with its mass spectrum resembling that of secondary organic aerosol (SOA). Pollution events (PEs) and clean periods (CPs) alternated routinely throughout the study. Secondary particulate matter (SPM = SOA + sulfate + nitrate + ammonium) dominated the total PM_1 mass on average, accounting for 63–82 % during nine PEs in this study. The elevated contributions of secondary species during PEs resulted in a higher mass extinction efficiency of PM_1 ($6.4\,m^2\,g^{-1}$) than during CPs ($4.4\,m^2\,g^{-1}$). The Chinese Spring Festival also provides a unique opportunity to study the impact of reduced anthropogenic emissions on aerosol chemistry in the city. Primary species showed ubiquitous reductions during the holiday period with the largest reduction being in cooking organic aerosol (OA; 69 %), in nitrogen monoxide (54 %), and in coal combustion OA (28 %). Secondary sulfate, however, remained only slightly changed, and the SOA and the total $PM_{2.5}$ even slightly increased. Our results have significant implications for controlling local primary source emissions during PEs, e.g., cooking and traffic activities. Controlling these factors might have a limited effect on improving air quality in the megacity of Beijing, due to the dominance of SPM from regional transport in aerosol particle composition.

1 Introduction

Air pollution caused by fine particles ($PM_{2.5}$) is of great concern in densely populated megacities because of its adverse effects on human health and regional air quality (Molina and Molina, 2004; Chan and Yao, 2008). The health risk of air pollution is greater than expected; it led to around 7 million deaths in 2012, according to the latest report by the World Health Organization (http://www.who.int/mediacentre/news/releases/2014/air-pollution/en/). The Beijing metropolitan area is one of the most populous megacities in the world, with the population having reached 20.69 million by the end of 2012 (Beijing Municipal Bureau of Statistics). According to the Beijing Municipal Environmental Protection Bureau, the annual average concentration of $PM_{2.5}$ was $89.5\,\mu g\,m^{-3}$ in 2013, which is about 2.5 times more than the National Ambient Air Quality Standards of China ($35\,\mu g\,m^{-3}$ for annual average). This suggests severe fine particle pollution in Beijing. Extensive studies have recently been carried out to investigate the chemical composition and sources of $PM_{2.5}$.

Results have shown that secondary inorganic aerosol (SIA = sulfate + nitrate + ammonium), coal combustion, traffic emissions (gasoline and diesel), biomass burning, cooking emissions, and dust are the major sources of $PM_{2.5}$ (Zheng et al., 2005; Song et al., 2006; Zhang et al., 2013). However, the source contributions were shown to vary significantly among different seasons; therefore improving air quality in Beijing remains a great challenge, due to the very complex sources and dynamic evolution processes of aerosol particles.

Fine particles from various sources can be either primary from direct emissions, e.g., fossil fuel combustion and biomass burning, or secondary from atmospheric oxidation of gas-phase species. Fireworks (FW) are one of the most important primary sources that can exert significant and short-time impacts on air quality. Their burning emits a large amount of gaseous pollutants, e.g., sulfur dioxide (SO_2) and nitrogen oxide (NO_x) (Vecchi et al., 2008; Huang et al., 2012), and also fine particles comprising organic/elemental carbon, sulfate, potassium, chloride, and various metals, e.g., copper (Cu), barium (Ba), strontium (Sr), and magnesium (Mg) (Moreno et al., 2007; Wang et al., 2007; Li et al., 2013). The enhanced short-term air pollution caused by fireworks can substantially increase health risk levels (Godri et al., 2010; Yang et al., 2014) and reduce visibility for hours (Vecchi et al., 2008). Previous studies on the chemical characterization of fireworks in China were mostly based on filter measurements, with a time resolution of 12 or 24 h (Wang et al., 2007; Zhang et al., 2010; Feng et al., 2012; Huang et al., 2012; Cheng et al., 2014; Zhao et al., 2014). Considering that FW events usually last less than 12 h, filter analysis may introduce large uncertainties in the accurate quantification of chemical composition of FW particles, due to either the interferences of non-FW (NFW) background aerosols or difficulties in accounting for meteorological variations. Drewnick et al. (2006) first conducted real-time size-resolved chemical composition measurements during the New Year period in Mainz, Germany, using an Aerodyne time-of-flight aerosol mass spectrometer (ToF-AMS). To our knowledge, there are as yet no such real-time measurements of the chemical composition of aerosol particles during firework events in China, which limits our understanding of the rapid formation and evolution of FW events, and of their impacts on particulate matter (PM) pollution.

Secondary aerosol is of more concern compared to primary aerosol because it is formed over a regional scale and exerts an impact on air quality over a wider area (Matsui et al., 2009; DeCarlo et al., 2010). Therefore, extensive studies have been conducted in recent years to characterize the sources and formation mechanisms of secondary aerosol (Yao et al., 2002; Duan et al., 2006; Sun et al., 2006, 2013b; Wang et al., 2006; Guo et al., 2010; Yang et al., 2011; Zhang et al., 2013; Zhao et al., 2013). SIA was observed to both contribute a large fraction of $PM_{2.5}$ and play an enhanced role during haze episodes, due to the faster heterogeneous reactions associated with higher humidity (Liu et al., 2013; Sun et al., 2013a, 2014; Zhao et al., 2013; Wang et al., 2014). While SIA has been relatively well characterized, secondary organic aerosol (SOA) is not well understood (Huang et al., 2014). Recent deployments of Aerodyne aerosol mass spectrometers (AMS) have greatly improved our understanding of the sources and evolution processes of OA (organic aerosol) in China, and also the different roles of primary organic aerosol (POA) and SOA in PM pollution (Huang et al., 2010; Sun et al., 2010, 2012, 2013b; He et al., 2011; Zhang et al., 2014). While SOA is more significant in summer (Huang et al., 2010; Sun et al., 2010, 2012), POA generally plays a more important role during wintertime (Sun et al., 2013b). Recently, the role of SOA in fine particle pollution during wintertime was extensively investigated; this is a season with frequent occurrences of pollution episodes in Beijing. The results highlighted the similar importance of SOA to SIA (Sun et al., 2013b, 2014; Zhang et al., 2014). However, the role of SOA in particulate pollution during periods with largely reduced anthropogenic activities was not yet well known (Huang et al., 2012). This study happened to take place in a month with the most important holiday in China, i.e., the Spring Festival. Source emissions (e.g., traffic and cooking) changed significantly due to a large decrease in population and anthropogenic activities in the city. This provides a unique opportunity to investigate how source changes affect aerosol chemistry, including primary emissions and secondary formation in Beijing. Although Huang et al. (2012) investigated such a holiday effect on aerosol composition and optical properties in Shanghai, the data analyses were limited by daily average composition measurements, and also the significantly different meteorological conditions between holiday and non-holiday periods.

In this study, an aerosol chemical speciation monitor (ACSM), along with various collocated instruments, was deployed in Beijing during February 2013. The chemical composition of submicron aerosol (PM_1) from fireworks is quantified based on the highly time-resolved measurements of non-refractory submicron aerosol (NR-PM_1) species (organics, sulfate nitrate, ammonium, chloride, and potassium) and black carbon. The impacts of FW on PM pollution during Chinese Lunar New Year (LNY), Lunar Fifth Day (LFD), and the Lantern Festival (LF) are investigated, and the roles of secondary formation in PM pollution are elucidated. Furthermore, the effects of reduced anthropogenic emissions on primary and secondary aerosols in the city are illustrated, which has significant implications for developing air pollution control strategies in Beijing.

2 Experimental method

2.1 Sampling site

The measurements in this study were conducted at the Institute of Atmospheric Physics (IAP), Chinese Academy of

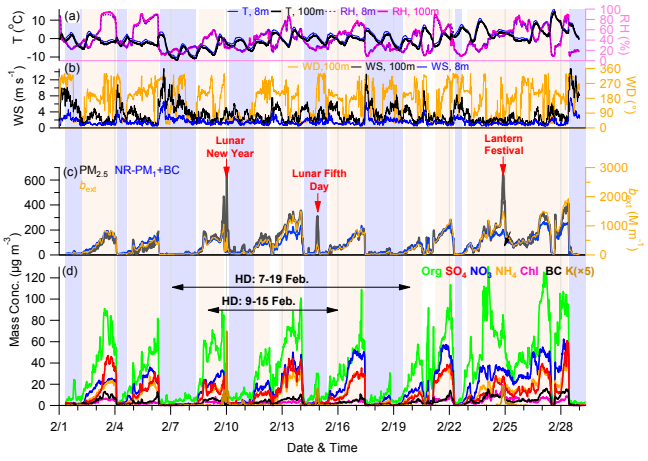

Figure 1. Time series of meteorological parameters: **(a)** relative humidity (RH) and temperature (T), **(b)** wind direction (WD) and wind speed (WS) at the height of 8 and 100 m, mass concentrations of **(c)** $PM_{2.5}$ and NR-PM_1 + BC, and **(d)** submicron aerosol species. The extinction coefficient (b_{ext}) at 630 nm is shown in **(c)**. Three events, i.e., LNY, LFD, and LF, with a significant influence of fireworks are marked in **(c)**. In addition, the classified clean periods (CPs) and polluted events (PEs) are marked as shaded light-blue and pink areas, respectively.

Sciences (39°58′28″ N, 116°22′16″ E), an urban site located between the north third and fourth ring road in Beijing (Sun et al., 2012). Aerosol measurements were performed from 1 February to 1 March 2013, when three episodes with a significant influence of fireworks, i.e., LNY, LFD, and LF, were observed (Fig. 1). The meteorological conditions during the measurement period are reported in Fig. 1. Winds at the ground surface were generally below 2 m s^{-1} and temperature averaged 0.6 °C. Relative humidity (RH) varied periodically, with higher values generally associated with higher PM pollution.

2.2 Aerosol sampling

The chemical composition of NR-PM_1, including organics, sulfate, nitrate, ammonium, and chloride, was measured in situ by the ACSM at approximately 15 min time intervals (Ng et al., 2011b). The ACSM has been widely used for long-term and routine aerosol particle composition measurements due to its robustness (Sun et al., 2012; Budisulistiorini et al., 2014; Petit et al., 2014), despite its lower sensitivity and mass resolution compared to previous versions of the research-grade AMS (Jayne et al., 2000; DeCarlo et al., 2006). In this study, the ambient air was drawn inside the sampling room at a flow rate of 3 L min^{-1}, of which ~ 0.1 L min^{-1} was subsampled into the ACSM and 0.85 L min^{-1} into a cavity-attenuated phase shift spectrometer (CAPS) particle extinction monitor (Massoli et al., 2010). A $PM_{2.5}$ cyclone (model: URG-2000-30ED) was supplied in front of the sampling line to remove coarse particles with aerodynamic diameters larger than 2.5 µm. The aerosol particles were dried by a silica gel dryer (RH < 40 %) before entering the ACSM and the CAPS. The ACSM was operated at a scan rate of 500 ms amu^{-1} for the mass spectrometer, between m/z 10–150. Because the ACSM cannot detect refractory components, e.g., BC and mineral dust, a two-wavelength Aethalometer (model AE22, Magee Scientific Corp.) was used to measure refractory BC in $PM_{2.5}$. The light extinction of dry fine particles (b_{ext}, 630 nm) was measured at a 1 s time resolution with a precision (3σ) of 1 M m^{-1} by the CAPS monitor. In addition, the mass concentration of $PM_{2.5}$ was determined by a heated tapered element oscillating microbalance (TEOM). The collocated gaseous species (including CO, SO_2, NO, NO_x, and O_3) were measured by various gas analyzers (Thermo Scientific) at a 1 min time resolution. A more detailed description of aerosol and gas measurements is given in Sun et al. (2013b). All the data in this study are reported in Beijing Standard Time.

2.3 ACSM data analysis

The ACSM data were analyzed for the mass concentrations and chemical composition of NR-PM_1 using standard ACSM software (v 1.5.3.2) written within Igor Pro (WaveMetrics, Inc., Oregon USA). A composition-dependent collection efficiency (CE) recommended by Middlebrook et al. (2012), CE = max (0.45, 0.0833 + 0.9167 × ANMF), was used to account for the incomplete detection due to the particle bouncing effects (Matthew et al., 2008) and the influences caused by high mass fraction of ammonium nitrate (ANMF). Because aerosol particles were overall neutralized ($NH_4^+{}_{measured}/NH_4^+{}_{predicted} = 1.01$, $r^2 = 0.99$) and also dried before entering the ACSM, the effects of particle acidity and RH were minor (Matthew et al., 2008; Middlebrook et al., 2012). The default relative ionization efficiencies (RIEs), except ammonium (RIE = 6.5) that was determined from the IE calibration, were used in this study. Quantification of K^+ is challenging when using an ACSM because of a large interference of organic $C_3H_3^+$ at m/z 39, and also because of uncertainties caused by surface ionization (Slowik et al., 2010). In this work, we found that m/z 39 was tightly correlated with m/z 43 that is completely organic during NFW periods ($r^2 = 0.87$, slope = 0.45, Fig. S1 in the Supplement). However, higher ratios of m/z 39/43 during FW periods were observed due to the elevated K^+ signal from the burning of FW. Assuming that m/z 39 was primarily contributed by organics during NFW periods, the excess m/z 39 signal, i.e., K^+, can then be estimated as m/z 39–m/z 43 × 0.45. The $^{41}K^+$ at m/z 41 was calculated using an isotopic ratio of 0.0722, i.e., $^{41}K^+ = 0.0722 \times K^+$. The K^+ signal was converted to mass concentration with a RIE of 2.9 that was reported by Drewnick et al. (2006). It should be noted that the quantification of K^+ in this study might have a large uncertainty because of the unknown RIE of K^+ (RIE_K). The RIE_K can vary a lot depending on the tuning of the spectrometer

and the temperature of the vaporizer. For example, Slowik et al. (2010) reported a $RIE_K = 10$, based on the calibration of pure KNO_3 particles using a ToF-AMS, which is much higher than the $RIE_K = 2.9$ obtained from the comparisons of K/S from fireworks and AMS measurements (Drewnick et al., 2006). In addition, the stability of surface ionization (SI) and electron impact (EI) also affects RIE_K. We then checked the variations of the ratio of $m/z\,39/m/z\,23$ (two m/z's with similar surface ionization issues). The average ratios of m/z 39/23 during LFD and LF are 8.7 and 11.1, respectively, which is close to 9.0 during NFW periods. The results suggest that the SI / EI ratio was relatively stable throughout the study. Because we did not have a collocated K measurement, $RIE_K = 2.9$ that was estimated from fireworks was used in this study. The quantified K^+ during LFD and LF contributed on average 4.5 and 4.7 % of PM_1, respectively, which is close to the ~ 5 % ($PM_{2.5}$) reported by Cheng et al. (2014). Also, the large contribution of K^+ to PM_1 (20.5 %) during LNY, likely due to the intensified firework emissions (mainly firecrackers), is consistent with that observed (17.3 %) during LNY 2014 in the megacity Tianjin (Tian et al., 2014). Using $RIE_K = 10$ will decrease the K^+ concentration by a factor of more than 3, which appears to underestimate K^+ a lot. Therefore, using $RIE_K = 2.9$ for the quantification of K^+ in our study appears to be reasonable. KCl^+ (m/z 74) and $^{41}KCl^+/K^{37}Cl^+$ (m/z 76) were estimated by the differences between measured and PMF-modeled m/z 74 (where PMF is the positive matrix factorization; Fig. S2). Not surprisingly, the quantified KCl^+ highly correlates with K^+ ($r^2 = 0.82$, Fig. S2c). The chloride concentration was also biased at m/z 35 during some periods (e.g., LNY, Fig. S3), which is likely due to the interferences of NaCl from fireworks. Therefore, Cl^+ (m/z 35) was recalculated based on its correlation with m/z 36 (mainly HCl^+ with negligible C_3^+ and ^{36}Ar), i.e., $m/z\,35 = 0.15 \times m/z\,36$. The $^{37}Cl^+$ was calculated using an isotopic ratio of 0.323, i.e., $^{37}Cl^+ = 0.323 \times {}^{35}Cl^+$. The comparison of the reconstructed chloride from the default values is shown in Fig. S3b.

The PMF with the algorithm of PMF2.exe in robust mode (Paatero and Tapper, 1994) was performed on OA mass spectra (m/z 12–120) to resolve distinct OA components from different sources. The PMF results were evaluated with an Igor Pro-based PMF evaluation tool (PET, v 2.04) (Ulbrich et al., 2009), following the procedures detailed in Zhang et al. (2011). After a careful evaluation of the spectral profiles, diurnal variations, and correlations with external tracers, a 6 factor solution ($Q/Q_{exp} = 4.3$) was chosen, yielding a hydrocarbon-like OA (HOA), a cooking OA (COA), a coal combustion OA (CCOA), and three oxygenated OA (OOA) components. Because of the absence of collocated measurements to validate the different OOA components, the three OOA components were recombined into one OOA component. The contributions of four OA factors were relatively stable across different fpeak values (average $\pm$ 1σ; min – max, Fig. S4): HOA (14 ± 1.6 %; 12–16 %), COA (14 ± 2.8 %; 11–17 %), CCOA (19 ± 2.7 %; 15–22 %), and OOA (51 ± 1.7; 49–55 %). However, considering the mass spectra of OA factors, fpeak $= -1$ presented the best correlation with those identified in winter 2011–2012 ($r^2 = 0.86$–0.99, Fig. S5) (Sun et al., 2013b); the four OA factors with fpeak $= -1$ were chosen in this study. The HOA spectrum resembles that identified by PMF analysis of high-resolution OA mass spectra in Beijing in January 2013 (Zhang et al., 2014), which are both characterized as pronounced m/z 91 and 115. Although the CCOA spectrum does not present similarly pronounced m/z's (e.g., 77, 91, 105, and 115) as those resolved at a rural site in central eastern China (Hu et al., 2013), it shows more similarity to those resolved in Beijing (Zhang et al., 2014). Also, CCOA correlates better with chloride as an importance source from coal combustion (Zhang et al., 2012) than with HOA ($r^2 = 0.41$ vs. 0.24), and it also correlates well with m/z 60 ($r^2 = 0.77$, Fig. S6), a tracer m/z for biomass burning (Cubison et al., 2011). Considering that the mass spectra and time series of HOA and CCOA are, overall, similar in this study, PMF analysis may still show uncertainties in differentiation of the two factors. In particular, ACSM does not measure high m/z's (> 150), which are crucial (e.g., PAH (polycyclic aromatic hydrocarbon) signals) for distinguishing HOA and CCOA. Because we did not have more external tracers to further validate these two factors, it was the best solution that we could obtain based on the current available data. Future work, such as performing high-resolution time-of-flight AMS measurements or PMF analysis with the multi-linear engine (ME-2) algorithm (Paatero, 1999), is needed for a better investigation of HOA and CCOA in urban Beijing during wintertime. The sum of HOA and CCOA correlates better with BC ($r^2 = 0.88$), NO_x ($r^2 = 0.77$), and CO ($r^2 = 0.63$) than it does with HOA ($r^2 = 0.36$–0.47), which might suggest that coal combustion emissions are also important sources of CO, BC, and NO_x during wintertime (Tian et al., 2008; Zhi et al., 2008). Although COA did not have external tracers to be validated by, it is very distinct, as suggested by its unique diurnal patterns (two peaks corresponding to meal times) and a high $m/z\,55/57$ ratio. Similar to our previous study (Sun et al., 2013b), the OOA shows a tight correlation with NO_3 ($r^2 = 0.90$), and also a good correlation with $SO_4^{2-} + NO_3^-$ ($r^2 = 0.87$). The mass spectral profiles and time series of four OA factors are shown in Fig. S6.

No biomass burning OA (BBOA) was resolved in this study. One of the reasons is that BBOA was likely not an important component of OA (e.g., < 5 %), which is unlikely to be resolved accurately by PMF (Ulbrich et al., 2009). Indeed, through checking the scatter plot of f_{60} vs. f_{44}, we observed no strong biomass burning influences throughout the study (Fig. S7). We found that f_{60} vs. f_{44} is outside of the typical biomass burning region(Cubison et al., 2011) for most of the time during this study. Although the average f_{60} (0.42 %) is

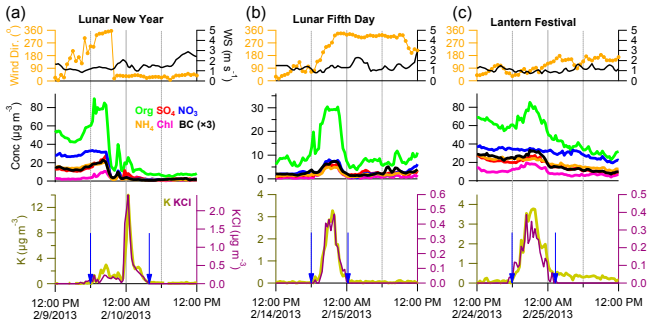

Figure 2. Time series of PM_1 species (Org, SO_4, NO_3, NH_4, Chl, K, KCl, and BC) and meteorological variables (wind direction (100 m) and wind speed (8 m)) during three firework events, i.e., **(a)** LNY, **(b)** LFD, and **(c)** LF. The two blue arrow lines represent the starting and ending times of firework events.

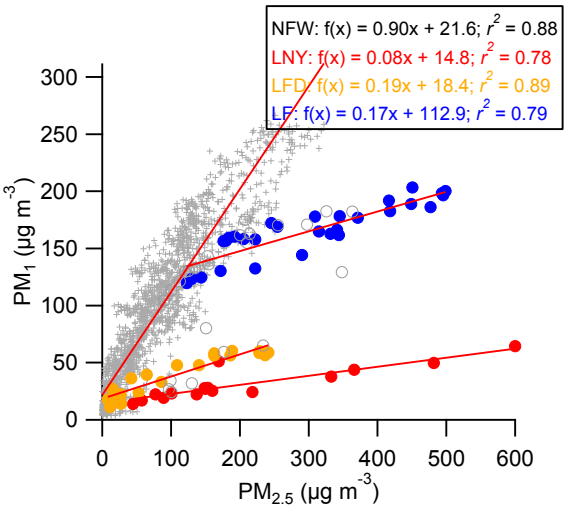

Figure 3. Correlation of PM_1 vs. $PM_{2.5}$ with the data segregated into three FW events (LNY, LFD, and LF), as well as NFW periods. The blank circles represent FW data between 18:00 and 23:30 on 9 February which were significantly influenced by NFW sources.

slightly higher than the typical value of f_{60} ($\sim 0.3\,\%$) in the absence of biomass burning impact (DeCarlo et al., 2008; Ulbrich et al., 2009), it is also likely due to the short range of m/z (12–120) used for the calculation of f_{60}. A summary of other key diagnostic plots of the PMF solution is given in Figs. S8 and S9.

3 Results and discussion

3.1 Identification and quantification of firework events

The burning of fireworks has been found to emit a large amount of K^+, which can be used to identify the FW events (Drewnick et al., 2006; Wang et al., 2007). As shown in Figs. 1 and 2, three FW events with significantly elevated K^+ were observed on the days of LNY (9–10 February), LFD (14 February), and LF (24 February), respectively. All three FW events started at approximately 18:00 and ended at midnight, except LNY which had a continuous FW impact until 04:00 the following day (Fig. 2). Figure 1 shows that the relative humidity was generally below 30 % during LNY and LFD. While the wind speed at the ground surface remained consistently below $2\,m\,s^{-1}$, it was increased to $\sim 4\,m\,s^{-1}$ at the height of 100 m. Also note that there was a change in wind direction in the middle of the two events. The meteorological conditions during LF were stagnant with wind speed generally below $2\,m\,s^{-1}$ across different heights. The relative humidity was $\sim 50\,\%$ and the temperature averaged 3.5 °C.

To estimate the contribution of fireworks, we first assume that the background concentration of each species has a linear variation during the FW period. A linear fit was therefore performed on the 6 h data before and after FW events. The difference between the measured and the fitted value is assumed as the contribution of FW. The typical examples for estimating FW contributions are shown in Fig. S10. It should be noted that this approach might significantly overestimate the FW contributions of primary species (e.g., HOA, COA, CCOA, and BC) that were largely enhanced during the typical FW periods (18:00–24:00), due to increased local emissions (see Fig. S11 for diurnal variations of aerosol species). However, it should have a minor impact on secondary species (e.g., SO_4, NO_3, and OOA) because of their relatively stable variations between 18:00 and 24:00. As shown in Fig. 2, all aerosol species showed substantial increases from 15:00 to 21:00 on the day of LNY, which coincidently corresponded to a gradual change in wind direction. Therefore, regional transport might have played a dominant role in the evolution of chemical species during this period. For these reasons, only FW contributions between 23:30 on 9 February and 03:30 on 10 February, when the meteorological conditions were stable, were estimated. FW contributions during LFD might also be overestimated due to the influences of regional transport, as suggested by the change in wind direction in the middle of the two events.

3.2 Mass concentration and chemical composition of FW aerosols

Figure 1 shows the time series of mass concentrations of PM_1, $PM_{2.5}$, and submicron aerosol species from 1 February to 1 March 2013. Because ACSM cannot measure the metals (e.g., Sr, Ba, Mg) that were significantly enhanced during FW periods (Wang et al., 2007; Vecchi et al., 2008), PM_1 in this study refers to NR-PM_1 (i.e., Org + SO_4 + NO_3 + NH_4 + Chl + K + KCl) + BC. $PM_{2.5}$ showed three prominent FW peaks with the maximum concentration occurring at $\sim$ 00:30 during LNY and $\sim$ 21:30 during LFD and LF. The peak concentration of $PM_{2.5}$ during LNY ($775\,\mu g\,m^{-3}$) is more than 10 times higher than the China National Ambient Air Quality

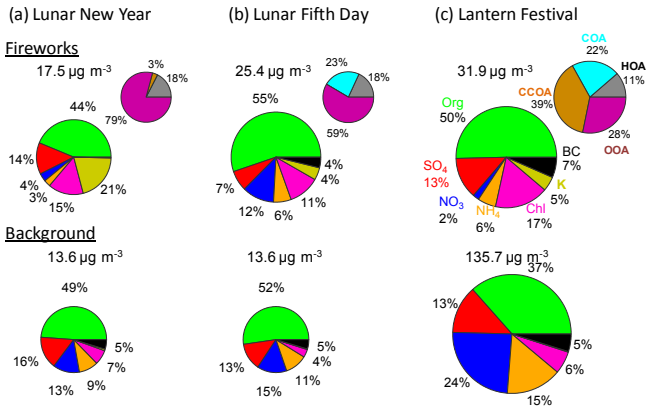

Figure 4. Average chemical composition of PM_1 and OA from fireworks and background conditions during three FW events.

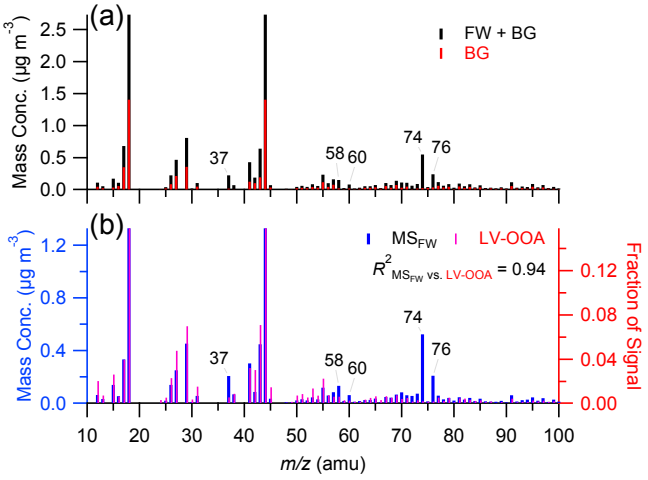

Figure 5. (a) Average mass spectra (MS) of OA during the firework period of Lunar New Year (23:30 on 9 February to 03:30 on 10 February) and the period of background (BG, 04:30–11:00, 10 February). **(b)** Comparison of the difference spectrum from **(a)**, i.e., MS_{FW+BG}–MS_{BG}, with the average LV-OOA spectrum in Ng et al. (2011a). Note that five m/z's – 37 ($^{37}Cl^+$), 58 ($NaCl^+$), 60 ($Na^{37}Cl^+$), 74 (KCl^+), and 76 ($K^{37}Cl^+$/ $^{41}KCl^+$) – marked in the figure were dominantly from the fragmentation of inorganic salts during fireworks.

Standard (75 μg m^{-3}, 24 h average). The average FW $PM_{2.5}$ mass concentrations during three FW events all exceeded 100 μg m^{-3}. These results suggest that fireworks have a large impact on fine particle pollution, but for generally less than half a day (approximately 10 h for LNY, and 6 h for LFD and LF). PM_1 also showed increases during the FW periods, although they were not as significant as $PM_{2.5}$. In fact, correlation of PM_1 versus $PM_{2.5}$ shows much lower PM_1 / $PM_{2.5}$ (0.08–0.19) ratios during three FW events than those observed during NFW periods (0.90) (Fig. 3). This is likely due to the mineral dust component and metals from fireworks that ACSM did not measure. However, the metals not detected by ACSM (e.g., Mg, Sr, and Ba) that are largely enhanced during FW periods generally contribute a small fraction of PM (< 2 %) (Wang et al., 2007; Vecchi et al., 2008; Kong et al., 2015). Therefore, our results might suggest that a large fraction of aerosol particles from the burning of fireworks was emitted in the size range of 1–2.5 μm. It is also possible that coagulations and condensation of VOCs on the aerosol phase during FW periods played a role. Vecchi et al. (2008) consistently found the best correlation between the fireworks tracer, Sr, and the particles between 700 and 800 nm (mobility diameter, D_m), which is approximately equivalent to 1.9–2.2 μm in D_{va} (vacuum aerodynamic diameter, D_{va}) with a density of 2.7 g cm^{-3} (Zhang et al., 2010).

Figure 4 shows the average chemical composition of PM_1 and OA from fireworks and also the background composition during LNY, LFD, and LF. The background PM_1 during LNY and LFD showed typical characteristics of clean periods with a high fraction of organics (> ∼ 50 %) (Sun et al., 2012, 2013b), whereas during LF it was dominated by SIA (52 %). As a comparison, organics constituted the major fraction of FW PM_1, contributing 44–55 % on average. During LNY, FW exerted a large impact on potassium and chloride, of which contributions were elevated to 21 and 15 % of PM_1, respectively, from less than 7 % (Chl) in the background aerosols. Large increases in potassium and chloride were also observed during LFD and LF, as in previous studies in Beijing (Wang et al., 2007; Cheng et al., 2014). As shown in Fig. 4, FW also emitted a considerable amount of sulfate, accounting for 7–14 % of PM_1. Sulfate correlated strongly with SO_2 during all three FW events ($r^2 = 0.49$–0.92). Given that the relative humidity was low, < 30 % during LNY and LFD, and ∼ 50 % during LF, aqueous-phase oxidation of SO_2 depending on liquid water content could not play a significant role in sulfate formation (Sun et al., 2013a). Therefore, sulfate in FW PM_1 was mainly from the direction emissions of FW. Compared to sulfate, FW appeared to show a minor impact on nitrate, for example, 4 and 2 % during LNY and LF, respectively. Although nitrate contributed 12 % of FW PM_1 during LFD, most of it was likely from regional transport, as supported by synchronous increases in all aerosol species, associated with a change in wind direction in the middle of the two events (Fig. 2).

The OOA contributed dominantly to OA during LNY: 79 % on average (Fig. 4a). As shown in Fig. 5, the mass spectrum of FW organics is highly similar to that of low-volatility OOA (LV OOA, $r^2 = 0.94$; $r^2 = 0.89$ by excluding m/z 18 and m/z 44) (Ng et al., 2011a), indicating that FW organics are likely emitted in secondary. Drewnick et al. (2006) also consistently found large enhancements of the OOA-related m/z's (e.g., m/z 44) during New Year fireworks, but the HOA-related m/z's (e.g., m/z 57) are not significant contributors to FW organics. OOA accounted for a much smaller fraction of OA during LF (28 %) due to the

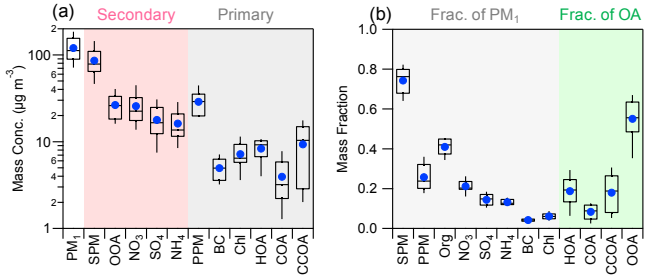

Figure 6. Box plots of **(a)** mass concentrations and **(b)** mass fractions of aerosol species for 9 pollution events marked in Fig. 1. The mean (blue circles), median (horizontal line), 25th and 75th percentiles (lower and upper box), and 10th and 90th percentiles (lower and upper whiskers) are shown for each box.

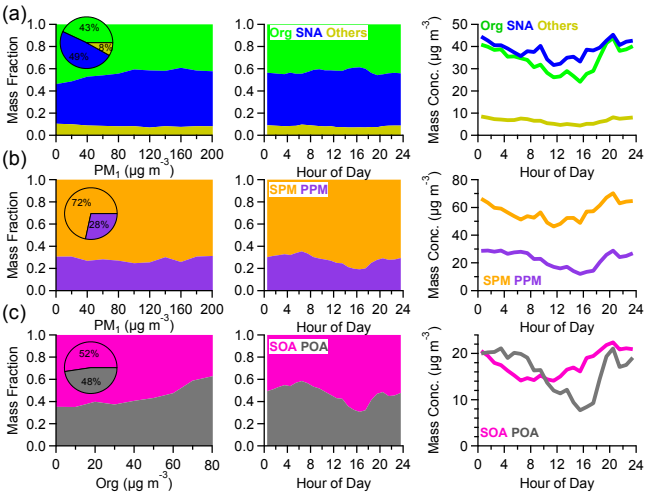

Figure 7. Left panels: variations in chemical composition of **(a)** organics, SNA (i.e., sulfate + nitrate + ammonium), and others (the rest species in PM_1), **(b)** SPM and PPM as a function of PM_1, and **(c)** SOA and POA as a function of organics loadings, respectively. The middle and right panels show the diurnal profiles of composition and mass concentrations, respectively.

large contributions of POA components (72 %). Although the OOA contributions varied during three FW events, their absolute concentrations were relatively close, ranging from 5.8 to 7.9 $\mu g\,m^{-3}$. It should be noted that our approach might overestimate the POA components in FW OA because of the influences of NFW sources, in particular during the FW period of LF, when the local HOA, COA, and CCOA happened to have large increases. By excluding the POA components in FW OA, FW contributed 15–19 $\mu g\,m^{-3}$ PM_1 on average during three FW events.

3.3 Secondary aerosol and PM pollution

The PM_1 (NR-PM_1 + BC) varied largely across the entire study with daily average mass concentration ranging from 9.1 to 169 $\mu g\,m^{-3}$. The average PM_1 mass concentration was 80 ($\pm$68) $\mu g\,m^{-3}$, which is approximately 20 % higher than observed during winter 2011–2012 (Sun et al., 2013b). Organics composed the major fraction of PM_1, accounting for 43 %, followed by nitrate (22 %), sulfate (14 %), ammonium (13 %), BC (5 %), and chloride (3 %). The OA composition was dominated by OOA (53 %), with the rest composed of POA. Compared to winter 2011–2012 (Sun et al., 2013b), this study showed significantly enhanced OOA (53 vs. 31 %) and secondary nitrate (22 vs. 16 %), indicating that secondary formation has played an important role in the formation of pollution episodes.

Figure 1d shows that submicron aerosol species alternated routinely between pollution events (PEs) and clean periods (CPs) throughout the entire study. The PEs generally lasted $\sim$1–2 days, except the one on 23–28 February that lasted more than 5 days, whereas the CPs were shorter, generally less than 1 day. In total, nine PEs and nine CPs were identified in this study (Fig. 1). A statistical diagram depicting the mass concentrations and mass fractions of aerosol species during nine PEs is presented in Fig. 6. The average PM_1 mass concentration ranged 68–179 $\mu g\,m^{-3}$ during PEs, with the total secondary particulate matter (SPM = OOA + SO_4 + NO_3 + NH_4) accounting for 63–82 %. The average mass concentration of SPM for the nine PEs was 86 ($\pm$32) $\mu g\,m^{-3}$, which is nearly 3 times that of primary PM (PPM = HOA + COA + CCOA + BC + Chl) (30 $\pm$ 9.5 $\mu g\,m^{-3}$). SPM consistently dominated PM_1 across different PM levels (69–75 %), but generally with higher contributions (up to 81 %) during daytime (Fig. 7b). The diurnal cycle of SPM presented a gradual increase from 50 to 70 $\mu g\,m^{-3}$ between 10:00 and 20:00, indicating evident photochemical production of secondary species during daytime. It should also be noted that all secondary species showed ubiquitously higher mass concentrations than those of primary species (Fig. 6a).

The SOA generally contributed more than 50 % to OA with an average of 55% during PEs except the episode on 3 February (35 %). It is interesting to note that the contribution of POA increased as a function of organic loadings, which varied from $\sim$35 to 63 % when organics were above 80 $\mu g\,m^{-3}$ (Fig. 7c). Such behavior is mainly caused by the enhanced CCOA at high organic mass loadings, which was also observed during winter 2011–2012 (Sun et al., 2013b). These results suggest that POA played a more important role than SOA in PM pollution during periods with high organic mass loadings (e.g., > 60 $\mu g\,m^{-3}$). In fact, POA showed even higher mass concentration than OOA at nighttime (00:00–08:00), due to intensified local emissions, e.g., coal combustion for heating. Despite this, the role of POA in PM pollution was compensated for by the elevated secondary inorganic species as a function of PM loadings (Fig. 7a), leading to consistently dominant SPM across different pollution levels. Figure 8a shows an evidently lower contribution of organics to PM_1 during PEs than during CPs. The elevated sec-

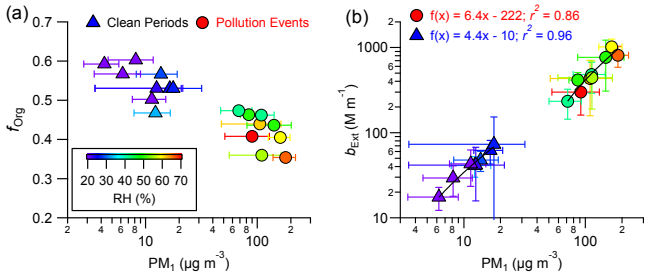

Figure 8. (a) Average mass fraction of organics (f_{Org}) as a function of PM_1 mass, and **(b)** correlations of extinction coefficients ($PM_{2.5}$) vs. PM_1 for nine PEs and nine CPs marked in Fig. 1. The error bar represents 1 standard deviation of the average for each event.

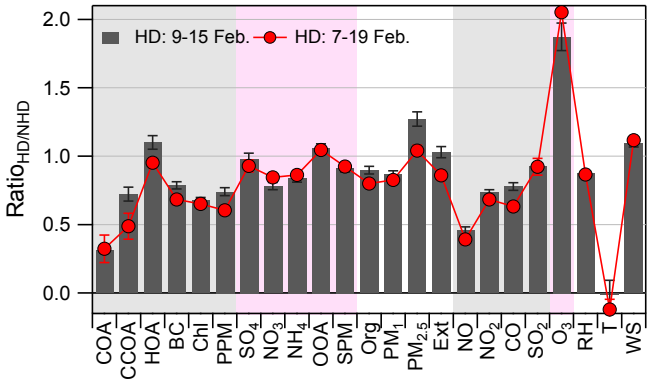

Figure 9. The average ratios of aerosol species, gaseous species, PM mass concentrations, extinction coefficient, and meteorological parameters between holiday (HD) and non-holiday (NHD) periods. Two different holidays, i.e., the official holiday of 9–15 February and the longer holiday of 7–20 February were used for averages. Also note that the averages were made by excluding clean periods and firework events during both HD and NHD days. The error bars are the standard errors of the ratios.

ondary inorganic species during PEs were closely related to the increase in RH (Fig. 1). For example, during the pollution episode on 3 February, the sulfate concentration increased rapidly and became a major inorganic species when RH increased from ∼ 60 % to > 90 %. Gaseous SO_2 showed a corresponding decrease, indicating aqueous-phase processing of SO_2 to form sulfate, consistent with our previous conclusion that aqueous-phase processing could have contributed more than 50 % of sulfate production during winter 2011–2012 (Sun et al., 2013a).

The compositional differences between PEs and CPs also led to different mass extinction efficiency (MEE; 630 nm) of PM_1 (Fig. 8b). The higher MEE (6.4 $m^2\,g^{-1}$) during PEs than in CPs (4.4 $m^2\,g^{-1}$) is primarily due to the enhanced secondary species, and is also likely due to increases in aerosol particle sizes, although we do not have size data to support this. Increases in mass scattering efficiency from CPs were similar in relatively polluted conditions; this was also observed previously in Beijing and Shanghai (Jung et al., 2009; Huang et al., 2013). It should be noted that the MEE of PM_1 in this study refers to $PM_{2.5}\,b_{ext}/PM_1$. Considering that PM_1 on average contributes ∼ 60–70 % of $PM_{2.5}$ in Beijing (Sun et al., 2012, 2013b), the real MEE of PM_1 during PEs and CPs would be ∼ 3.8–4.5 and ∼ 2.6–3.1 $m^2\,g^{-1}$, respectively.

3.4 Holiday effects on PM pollution

Figure 9 shows a comparison of aerosol species, gaseous species, and meteorological parameters between holiday (HD) and non-holiday (NHD) periods. The official holiday for the Spring Festival was 9–15 February. However, we noted a large decrease in cooking aerosols from 7 February until 19 February (Fig. S6b), of which emissions were expected to be stable under similar meteorological conditions. The decrease in COA was likely due to a decrease in the population in Beijing, which corresponded with the fact that most migrants from outside Beijing were leaving for their hometown before the official holiday. Therefore, 7–19 February was used as a longer holiday for comparison. It was estimated that approximately half of the population (9 million) left Beijing before the Spring Festival (http://news.xinhuanet.com/yzyd/local/20130208/c_114658765.htm). Such a great decrease in human activity would exert a large impact on aerosol composition and sources in the city during holidays. To better investigate HD effects on PM pollution, the data shown in Fig. 9 excluded the CPs marked in Fig. 1. The data with the CPs included are presented in Fig. S12.

The differences between HD and NHD for primary species varied largely among different species. COA showed the largest reduction (69 %) among aerosol species, with the average concentration decreasing from 5.8 μg m^{-3} during NHD to 1.8 μg m^{-3} during HD. The contribution of COA to OA showed a corresponding decrease from 12 to 4 %. Given the similar meteorological conditions between HD and NHD, e.g., RH (46 vs. 52 %) and wind speed (1.3 m s^{-1} vs. 1.2 m s^{-1}), the reduction in COA clearly indicated a large decrease in population and in the number of restaurants opened during HD. CCOA showed an approximately 30 % reduction during HD, and its contribution to OA decreased from 23 to 18 %. Not surprisingly, chloride showed a similar reduction to CCOA because it was primarily from coal combustion emissions during wintertime (Sun et al., 2013b). Figure 9 also shows a significant reduction (54 %) for NO, indicating much fewer traffic emissions in the city during HD. HOA, however, even showed a slight increase during HD, which appears to be in contradiction with the reduction in two combustion-related tracers, BC and CO (∼ 20 %). This can be explained by the fact that coal combustion is a large source of BC and CO during the heating season (Tian et al., 2008; Zhi et al., 2008). Consequently, BC and CO showed relatively similar reductions in CCOA. Therefore, the minor variation in HOA might indicate that the num-

ber of heavy-duty vehicles and diesel trucks that dominated HOA emissions (Massoli et al., 2012; Hayes et al., 2013) remained slightly changed during the HD period, although the amount of HOA emissions of gasoline vehicles was largely decreased. It should be noted that HOA showed a large peak on 9 February – the first day of the official holiday (Fig. S6b), when more traffic emissions were expected due to many people leaving for their hometown. After that, HOA showed a slightly lower concentration during 11–17 February than other periods. In fact, average HOA showed a slight reduction ($\sim 5\,\%$) during the longer holiday period (7–19 February), suggesting a small effect of the holiday on HOA reduction. Together, the total primary aerosol species (PPM) showed an average reduction of 22 % because of holiday effects.

Nitrate showed the largest reduction among secondary species by 22 % during HD, primarily due to a reduction in its precursors NO and NO_2. The results suggest that reducing traffic emissions would help mitigate the nitrate pollution in the city. Compared to nitrate, sulfate showed minor changes (2 %) between HD and NHD, and OOA even showed a slight increase (6 %) during HD. One of the reasons is that secondary sulfate and OOA were mainly formed over a regional scale and were less affected by local production, consistent with their relatively flat diurnal cycles (Fig. S11). Ammonium showed a reduction between nitrate and sulfate because ammonium mainly existed in the form of $(NH_4)_2SO_4$ and NH_4NO_3. Overall, secondary species showed generally lower reductions than primary species, with the total secondary species (SPM) showing an average reduction of 9 % during HD. The joint reductions of PPM and SPM led to an average reduction of 13 % for PM_1 during HD. However, these reductions did not help alleviate the fine particle pollution during HD. The $PM_{2.5}$, excluding FW impact, even showed a 27 % increase from 96 $\mu g\,m^{-3}$ during NHD to 122 $\mu g\,m^{-3}$ during HD. One possible reason is likely due to the increase in aerosol species in the size range of 1–2.5 µm during HD period. The longer holiday (LHD, 7–19 February) showed influences on both primary and secondary species similar to in the official holiday (9–15 February). COA, CCOA, and NO are the three species with the largest reductions during LHD ($> 50\,\%$). However, HOA, SO_4, OOA, and $PM_{2.5}$ showed rather small changes ($< \pm 7\,\%$). Therefore, results in this study suggest that controlling the primary source emissions, e.g., cooking and traffic emissions, in the city can reduce the primary particles largely, yet this has limited effects on secondary species and the total fine particle mass. One of the reasons is because the severe PM pollution in Beijing is predominantly contributed to by secondary species (see discussions in Sect. 3.3) that are formed over regional scales. Reducing the primary source emissions in local areas would have a limited impact on the mitigation of air pollution in the city. Similarly, Guo et al. (2013) reported a large reduction in primary organic carbon (OC) from traffic emissions and coal combustion during the 2008 Olympic Summer Games, when traffic restrictions and temporary closure of factories were implemented. However, secondary OC was not statistically different between controlled and non-controlled periods. Our results highlight the importance of implementing joint efforts over a regional scale for air pollution control in north China.

4 Conclusions

We have characterized the aerosol particle composition and sources during the Chinese Spring Festival in 2013. The average PM_1 mass concentration was 80 (± 68) $\mu g\,m^{-3}$ for the entire study, with organics being the major fraction (43 %). Nine PEs and nine CPs with substantial compositional differences were observed. SPM (i.e., SOA+ sulfate + nitrate + ammonium) played a dominant role in PM pollution during nine PEs. The contributions of SPM to PM_1 varied from 63 to 82 % with SOA, on average, accounting for $\sim 55\,\%$ of OA. As a result, the average mass extinction efficiency of PM_1 during PEs (6.4 $m^2\,g^{-1}$) was higher than that during CPs (4.4 $m^2\,g^{-1}$). Three FW events, i.e., LNY, LFD, and LF, were identified, which showed significant and short-term impacts on fine particles, as well as non-refractory potassium, chloride, and sulfate in PM_1. FW also exerted a large impact on organics that were mainly demonstrated as secondary, as indicated by its similar mass spectrum to that of oxygenated OA. The holiday effects on aerosol composition and sources were also investigated by comparing the differences between holiday and non-holiday periods. The changes in anthropogenic source emissions during the holiday showed large impacts on reduction of cooking OA (69 %), nitrogen monoxide (54 %), and coal combustion OA (28 %) in the city, yet presented much smaller influences on secondary species. The average SOA and the total $PM_{2.5}$ even increased slightly during the holiday period. Results here have significant implications for controlling local primary source emissions, e.g., cooking and traffic activities. Controlling these factors might have a limited effect on improving air quality during polluted days, when SPM from regional transport dominated aerosol composition for most of the time. Our results also highlight the importance of implementing joint measures over a regional scale for the mitigation of air pollution in the megacity Beijing.

The Supplement related to this article is available online at doi:10.5194/acp-15-6023-2015-supplement.

Acknowledgements. This work was supported by the National Key Project of Basic Research (2014CB447900, 2013CB955801), the Strategic Priority Research Program (B) of the Chinese Academy

of Sciences (grant no. XDB05020501), and the National Natural Science Foundation of China (41175108). We thank Huabin Dong, Hongyan Chen, and Zhe Wang for their help with the data collection, and also the Technical and Service Center, Institute of Atmospheric Physics, and the Chinese Academy of Sciences for providing meteorological data.

Edited by: Y. Cheng

References

Budisulistiorini, S. H., Canagaratna, M. R., Croteau, P. L., Baumann, K., Edgerton, E. S., Kollman, M. S., Ng, N. L., Verma, V., Shaw, S. L., Knipping, E. M., Worsnop, D. R., Jayne, J. T., Weber, R.J., and Surratt, J. D.: Intercomparison of an Aerosol Chemical Speciation Monitor (ACSM) with ambient fine aerosol measurements in downtown Atlanta, Georgia, Atmos. Meas. Tech., 7, 1929–1941, doi:10.5194/amt-7-1929-2014, 2014.

Chan, C. K. and Yao, X.: Air pollution in mega cities in China, Atmos. Environ., 42, 1–42, doi:10.1016/j.atmosenv.2007.09.003, 2008.

Cheng, Y., Engling, G., He, K.-B., Duan, F.-K., Du, Z.-Y., Ma, Y.-L., Liang, L.-L., Lu, Z.-F., Liu, J.-M., Zheng, M., and Weber, R. J.: The characteristics of Beijing aerosol during two distinct episodes: Impacts of biomass burning and fireworks, Environ. Pollut., 185, 149–157, doi:10.1016/j.envpol.2013.10.037, 2014.

Cubison, M. J., Ortega, A. M., Hayes, P. L., Farmer, D. K., Day, D., Lechner, M. J., Brune, W. H., Apel, E., Diskin, G. S., Fisher, J. A., Fuelberg, H. E., Hecobian, A., Knapp, D. J., Mikoviny, T., Riemer, D., Sachse, G. W., Sessions, W., Weber, R. J., Weinheimer, A. J., Wisthaler, A., and Jimenez, J. L.: Effects of aging on organic aerosol from open biomass burning smoke in aircraft and laboratory studies, Atmos. Chem. Phys., 11, 12049–12064, doi:10.5194/acp-11-12049-2011, 2011.

DeCarlo, P. F., Kimmel, J. R., Trimborn, A., Northway, M. J., Jayne, J. T., Aiken, A. C., Gonin, M., Fuhrer, K., Horvath, T., Docherty, K. S., Worsnop, D. R., and Jimenez, J. L.: Field-Deployable, High-Resolution, Time-of-Flight Aerosol Mass Spectrometer, Anal. Chem., 78, 8281–8289, 2006.

DeCarlo, P. F., Dunlea, E. J., Kimmel, J. R., Aiken, A. C., Sueper, D., Crounse, J., Wennberg, P. O., Emmons, L., Shinozuka, Y., Clarke, A., Zhou, J., Tomlinson, J., Collins, D. R., Knapp, D., Weinheimer, A. J., Montzka, D. D., Campos, T., and Jimenez, J. L.: Fast airborne aerosol size and chemistry measurements above Mexico City and Central Mexico during the MILAGRO campaign, Atmos. Chem. Phys., 8, 4027–4048, doi:10.5194/acp-8-4027-2008, 2008.

DeCarlo, P. F., Ulbrich, I. M., Crounse, J., de Foy, B., Dunlea, E. J., Aiken, A. C., Knapp, D., Weinheimer, A. J., Campos, T., Wennberg, P. O., and Jimenez, J. L.: Investigation of the sources and processing of organic aerosol over the Central Mexican Plateau from aircraft measurements during MILAGRO, Atmos. Chem. Phys., 10, 5257–5280, doi:10.5194/acp-10-5257-2010, 2010.

Drewnick, F., Hings, S. S., Curtius, J., Eerdekens, G., and Williams, J.: Measurement of fine particulate and gas-phase species during the New Year's fireworks 2005 in Mainz, Germany, Atmos. Environ., 40, 4316–4327, doi:10.1016/j.atmosenv.2006.03.040, 2006.

Duan, F. K., He, K. B., Ma, Y. L., Yang, F. M., Yu, X. C., Cadle, S. H., Chan, T., and Mulawa, P. A.: Concentration and chemical characteristics of $PM_{2.5}$ in Beijing, China: 2001–2002, Sci. Total Environ., 355, 264–275, doi:10.1016/j.scitotenv.2005.03.001, 2006.

Feng, J., Sun, P., Hu, X., Zhao, W., Wu, M., and Fu, J.: The chemical composition and sources of PM2.5 during the 2009 Chinese New Year's holiday in Shanghai, Atmos. Res., 118, 435–444, doi:10.1016/j.atmosres.2012.08.012, 2012.

Godri, K. J., Green, D. C., Fuller, G. W., Dall'Osto, M., Beddows, D. C., Kelly, F. J., Harrison, R. M., and Mudway, I. S.: Particulate oxidative burden associated with firework activity, Environ. Sci. Technol., 44, 8295–8301, 2010.

Guo, S., Hu, M., Wang, Z. B., Slanina, J., and Zhao, Y. L.: Size-resolved aerosol water-soluble ionic compositions in the summer of Beijing: implication of regional secondary formation, Atmos. Chem. Phys., 10, 947–959, doi:10.5194/acp-10-947-2010, 2010.

Guo, S., Hu, M., Guo, Q., Zhang, X., Schauer, J. J., and Zhang, R.: Quantitative evaluation of emission controls on primary and secondary organic aerosol sources during Beijing 2008 Olympics, Atmos. Chem. Phys., 13, 8303–8314, doi:10.5194/acp-13-8303-2013, 2013.

Hayes, P. L., Ortega, A. M., Cubison, M. J., Froyd, K. D., Zhao, Y., Cliff, S. S., Hu, W. W., Toohey, D. W., Flynn, J. H., Lefer, B. L., Grossberg, N., Alvarez, S., Rappenglück, B., Taylor, J. W., Allan, J. D., Holloway, J. S., Gilman, J. B., Kuster, W. C., de Gouw, J. A., Massoli, P., Zhang, X., Liu, J., Weber, R. J., Corrigan, A. L., Russell, L. M., Isaacman, G., Worton, D. R., Kreisberg, N. M., Goldstein, A. H., Thalman, R., Waxman, E. M., Volkamer, R., Lin, Y. H., Surratt, J. D., Kleindienst, T. E., Offenberg, J. H., Dusanter, S., Griffith, S., Stevens, P. S., Brioude, J., Angevine, W. M., and Jimenez, J. L.: Organic aerosol composition and sources in Pasadena, California during the 2010 CalNex campaign, J. Geophys. Res.-Atmos., 118, 9233–9257, 10.1002/jgrd.50530, 2013.

He, L.-Y., Huang, X.-F., Xue, L., Hu, M., Lin, Y., Zheng, J., Zhang, R., and Zhang, Y.-H.: Submicron aerosol analysis and organic source apportionment in an urban atmosphere in Pearl River Delta of China using high-resolution aerosol mass spectrometry, J. Geophys. Res., 116, D12304, doi:10.1029/2010jd014566, 2011.

Hu, W. W., Hu, M., Yuan, B., Jimenez, J. L., Tang, Q., Peng, J. F., Hu, W., Shao, M., Wang, M., Zeng, L. M., Wu, Y. S., Gong, Z. H., Huang, X. F., and He, L. Y.: Insights on organic aerosol aging and the influence of coal combustion at a regional receptor site of central eastern China, Atmos. Chem. Phys., 13, 10095–10112, doi:10.5194/acp-13-10095-2013, 2013.

Huang, K., Zhuang, G., Lin, Y., Wang, Q., Fu, J. S., Zhang, R., Li, J., Deng, C., and Fu, Q.: Impact of anthropogenic emission on air quality over a megacity – revealed from an intensive atmospheric campaign during the Chinese Spring Festival, Atmos. Chem. Phys., 12, 11631–11645, doi:10.5194/acp-12-11631-2012, 2012.

Huang, R.-J., Zhang, Y., Bozzetti, C., Ho, K.-F., Cao, J.-J., Han, Y., Daellenbach, K. R., Slowik, J. G., Platt, S. M., Canonaco, F., Zotter, P., Wolf, R., Pieber, S. M., Bruns, E. A., Crippa, M., Ciarelli, G., Piazzalunga, A., Schwikowski, M., Abbaszade, G., Schnelle-Kreis, J., Zimmermann, R., An, Z., Szidat, S., Baltensperger, U., Haddad, I. E., and Prevot, A. S. H.: High secondary aerosol con-

tribution to particulate pollution during haze events in China, Nature, 514, 218–222, doi:10.1038/nature13774, 2014.

Huang, X.-F., He, L.-Y., Hu, M., Canagaratna, M. R., Sun, Y., Zhang, Q., Zhu, T., Xue, L., Zeng, L.-W., Liu, X.-G., Zhang, Y.-H., Jayne, J. T., Ng, N. L., and Worsnop, D. R.: Highly time-resolved chemical characterization of atmospheric submicron particles during 2008 Beijing Olympic Games using an Aerodyne High-Resolution Aerosol Mass Spectrometer, Atmos. Chem. Phys., 10, 8933–8945, doi:10.5194/acp-10-8933-2010, 2010.

Huang, Y., Li, L., Li, J., Wang, X., Chen, H., Chen, J., Yang, X., Gross, D. S., Wang, H., Qiao, L., and Chen, C.: A case study of the highly time-resolved evolution of aerosol chemical and optical properties in urban Shanghai, China, Atmos. Chem. Phys., 13, 3931–3944, doi:10.5194/acp-13-3931-2013, 2013.

Jayne, J. T., Leard, D. C., Zhang, X., Davidovits, P., Smith, K. A., Kolb, C. E., and Worsnop, D. R.: Development of an aerosol mass spectrometer for size and composition analysis of submicron particles, Aerosol Sci. Tech., 33, 49–70, 2000.

Jung, J., Lee, H., Kim, Y. J., Liu, X., Zhang, Y., Hu, M., and Sugimoto, N.: Optical properties of atmospheric aerosols obtained by in situ and remote measurements during 2006 Campaign of Air Quality Research in Beijing (CAREBeijing-2006), J. Geophys. Res., 114, D00G02, doi:10.1029/2008jd010337, 2009.

Kong, S. F., Li, L., Li, X. X., Yin, Y., Chen, K., Liu, D. T., Yuan, L., Zhang, Y. J., Shan, Y. P., and Ji, Y. Q.: The impacts of firework burning at the Chinese Spring Festival on air quality: insights of tracers, source evolution and aging processes, Atmos. Chem. Phys., 15, 2167–2184, doi:10.5194/acp-15-2167-2015, 2015.

Li, W., Shi, Z., Yan, C., Yang, L., Dong, C., and Wang, W.: Individual metal-bearing particles in a regional haze caused by firecracker and firework emissions, Sci. Total Environ., 443, 464–469, doi:10.1016/j.scitotenv.2012.10.109, 2013.

Liu, X. G., Li, J., Qu, Y., Han, T., Hou, L., Gu, J., Chen, C., Yang, Y., Liu, X., Yang, T., Zhang, Y., Tian, H., and Hu, M.: Formation and evolution mechanism of regional haze: a case study in the megacity Beijing, China, Atmos. Chem. Phys., 13, 4501–4514, doi:10.5194/acp-13-4501-2013, 2013.

Massoli, P., Kebabian, P. L., Onasch, T. B., Hills, F. B., and Freedman, A.: Aerosol light extinction measurements by Cavity Attenuated Phase Shift (CAPS) spectroscopy: Laboratory validation and field deployment of a compact aerosol particle extinction monitor, Aerosol Sci. Tech., 44, 428–435, doi:10.1080/02786821003716599, 2010.

Massoli, P., Fortner, E. C., Canagaratna, M. R., Williams, L. R., Zhang, Q., Sun, Y., Schwab, J. J., Trimborn, A., Onasch, T. B., Demerjian, K. L., Kolb, C. E., Worsnop, D. R., and Jayne, J. T.: Pollution gradients and chemical characterization of particulate matter from vehicular traffic near major roadways: Results from the 2009 Queens College Air Quality Study in NYC, Aerosol Sci. Tech., 46, 1201–1218, doi:10.1080/02786826.2012.701784, 2012.

Matsui, H., Koike, M., Kondo, Y., Takegawa, N., Kita, K., Miyazaki, Y., Hu, M., Chang, S. Y., Blake, D. R., Fast, J. D., Zaveri, R. A., Streets, D. G., Zhang, Q., and Zhu, T.: Spatial and temporal variations of aerosols around Beijing in summer 2006: Model evaluation and source apportionment, J. Geophys. Res., 114, D00G13, doi:10.1029/2008jd010906, 2009.

Matthew, B. M., Middlebrook, A. M., and Onasch, T. B.: Collection Efficiencies in an Aerodyne Aerosol Mass Spectrometer as a Function of Particle Phase for Laboratory Generated Aerosols, Aerosol Sci. Tech., 42, 884–898, 2008.

Middlebrook, A. M., Bahreini, R., Jimenez, J. L., and Canagaratna, M. R.: Evaluation of composition-dependent collection efficiencies for the Aerodyne Aerosol Mass Spectrometer using field data, Aerosol Sci. Tech., 46, 258–271, 2012.

Molina, M. J. and Molina, L. T.: Megacities and atmospheric pollution, J. Air Waste Manage. Assoc., 54, 644–680, 2004.

Moreno, T., Querol, X., Alastuey, A., Cruz Minguillón, M., Pey, J., Rodriguez, S., Vicente Miró, J., Felis, C., and Gibbons, W.: Recreational atmospheric pollution episodes: Inhalable metalliferous particles from firework displays, Atmos. Environ., 41, 913–922, doi:10.1016/j.atmosenv.2006.09.019, 2007.

Ng, N. L., Canagaratna, M. R., Jimenez, J. L., Zhang, Q., Ulbrich, I. M., and Worsnop, D. R.: Real-time methods for estimating organic component mass concentrations from Aerosol Mass Spectrometer data, Environ. Sci. Technol., 45, 910–916, doi:10.1021/es102951k, 2011a.

Ng, N. L., Herndon, S. C., Trimborn, A., Canagaratna, M. R., Croteau, P. L., Onasch, T. B., Sueper, D., Worsnop, D. R., Zhang, Q., Sun, Y. L., and Jayne, J. T.: An Aerosol Chemical Speciation Monitor (ACSM) for routine monitoring of the composition and mass concentrations of ambient aerosol, Aerosol Sci. Tech., 45, 770–784, 2011b.

Paatero, P. and Tapper, U.: Positive matrix factorization: A non-negative factor model with optimal utilization of error estimates of data values, Environmetrics, 5, 111–126, 1994.

Paatero, P.: The multilinear engine – A table-driven, least squares program for solving multilinear problems, including the n-way parallel factor analysis model, J. Comput. Graph. Stat., 8, 854–888, 1999.

Petit, J.-E., Favez, O., Sciare, J., Canonaco, F., Croteau, P., Mocnik, G., Jayne, J., Worsnop, D., and Leoz-Garziandia, E.: Submicron aerosol source apportionment of wintertime pollution in Paris, France by double positive matrix factorization (PMF2) using an aerosol chemical speciation monitor (ACSM) and a multi-wavelength Aethalometer, Atmos. Chem. Phys., 14, 13773–13787, doi:10.5194/acp-14-13773-2014, 2014.

Slowik, J. G., Stroud, C., Bottenheim, J. W., Brickell, P. C., Chang, R. Y.-W., Liggio, J., Makar, P. A., Martin, R. V., Moran, M. D., Shantz, N. C., Sjostedt, S. J., van Donkelaar, A., Vlasenko, A., Wiebe, H. A., Xia, A. G., Zhang, J., Leaitch, W. R., and Abbatt, J. P. D.: Characterization of a large biogenic secondary organic aerosol event from eastern Canadian forests, Atmos. Chem. Phys., 10, 2825–2845, doi:10.5194/acp-10-2825-2010, 2010.

Song, Y., Zhang, Y., Xie, S., Zeng, L., Zheng, M., Salmon, L. G., Shao, M., and Slanina, S.: Source apportionment of $PM_{2.5}$ in Beijing by positive matrix factorization, Atmos. Environ., 40, 1526–1537, doi:10.1016/j.atmosenv.2005.10.039, 2006.

Sun, J., Zhang, Q., Canagaratna, M. R., Zhang, Y., Ng, N. L., Sun, Y., Jayne, J. T., Zhang, X., Zhang, X., and Worsnop, D. R.: Highly time- and size-resolved characterization of submicron aerosol particles in Beijing using an Aerodyne Aerosol Mass Spectrometer, Atmos. Environ., 44, 131–140, 2010.

Sun, Y., Zhuang, G., Tang, A., Wang, Y., and An, Z.: Chemical Characteristics of $PM_{2.5}$ and PM_{10} in Haze-Fog Episodes in Beijing, Environ. Sci. Technol., 40, 3148–3155, 2006.

Sun, Y. L., Wang, Z., Dong, H., Yang, T., Li, J., Pan, X., Chen, P., and Jayne, J. T.: Characterization of summer organic and inorganic aerosols in Beijing, China with an Aerosol Chemical Speciation Monitor, Atmos. Environ., 51, 250–259, doi:10.1016/j.atmosenv.2012.01.013, 2012.

Sun, Y. L., Wang, Z., Fu, P., Jiang, Q., Yang, T., Li, J., and Ge, X.: The impact of relative humidity on aerosol composition and evolution processes during wintertime in Beijing, China, Atmos. Environ., 77, 927–934, doi:10.1016/j.atmosenv.2013.06.019, 2013a.

Sun, Y. L., Wang, Z. F., Fu, P. Q., Yang, T., Jiang, Q., Dong, H. B., Li, J., and Jia, J. J.: Aerosol composition, sources and processes during wintertime in Beijing, China, Atmos. Chem. Phys., 13, 4577–4592, doi:10.5194/acp-13-4577-2013, 2013b.

Sun, Y. L., Jiang, Q., Wang, Z., Fu, P., Li, J., Yang, T., and Yin, Y.: Investigation of the sources and evolution processes of severe haze pollution in Beijing in January 2013, J. Geophys. Res., 119, 4380–4398, doi:10.1002/2014JD021641, 2014.

Tian, L., Lucas, D., Fischer, S. L., Lee, S. C., Hammond, S. K., and Koshland, C. P.: Particle and Gas Emissions from a Simulated Coal-Burning Household Fire Pit, Environ. Sci. Technol., 42, 2503–2508, doi:10.1021/es0716610, 2008.

Tian, Y. Z., Wang, J., Peng, X., Shi, G. L., and Feng, Y. C.: Estimation of the direct and indirect impacts of fireworks on the physicochemical characteristics of atmospheric PM10 and PM2.5, Atmos. Chem. Phys., 14, 9469–9479, doi:10.5194/acp-14-9469-2014, 2014.

Ulbrich, I. M., Canagaratna, M. R., Zhang, Q., Worsnop, D. R., and Jimenez, J. L.: Interpretation of organic components from Positive Matrix Factorization of aerosol mass spectrometric data, Atmos. Chem. Phys., 9, 2891–2918, doi:10.5194/acp-9-2891-2009, 2009.

Vecchi, R., Bernardoni, V., Cricchio, D., D'Alessandro, A., Fermo, P., Lucarelli, F., Nava, S., Piazzalunga, A., and Valli, G.: The impact of fireworks on airborne particles, Atmos. Environ., 42, 1121–1132, doi:10.1016/j.atmosenv.2007.10.047, 2008.

Wang, Y., Zhuang, G., Sun, Y., and An, Z.: The variation of characteristics and formation mechanisms of aerosols in dust, haze, and clear days in Beijing, Atmos. Environ., 40, 6579–6591, 2006.

Wang, Y., Zhuang, G., Xu, C., and An, Z.: The air pollution caused by the burning of fireworks during the lantern festival in Beijing, Atmos. Environ., 41, 417–431, doi:10.1016/j.atmosenv.2006.07.043, 2007.

Wang, Y., Yao, L., Wang, L., Liu, Z., Ji, D., Tang, G., Zhang, J., Sun, Y., Hu, B., and Xin, J.: Mechanism for the formation of the January 2013 heavy haze pollution episode over central and eastern China, Sci. China Earth Sci., 57, 14–25, doi:10.1007/s11430-013-4773-4, 2014.

Yang, F., Tan, J., Zhao, Q., Du, Z., He, K., Ma, Y., Duan, F., Chen, G., and Zhao, Q.: Characteristics of $PM_{2.5}$ speciation in representative megacities and across China, Atmos. Chem. Phys., 11, 5207–5219, doi:10.5194/acp-11-5207-2011, 2011.

Yang, L., Gao, X., Wang, X., Nie, W., Wang, J., Gao, R., Xu, P., Shou, Y., Zhang, Q., and Wang, W.: Impacts of firecracker burning on aerosol chemical characteristics and human health risk levels during the Chinese New Year Celebration in Jinan, China, Sci. Total Environ., 476–477, 57–64, doi:10.1016/j.scitotenv.2013.12.110, 2014.

Yao, X., Chan, C. K., Fang, M., Cadle, S., Chan, T., Mulawa, P., He, K., and Ye, B.: The water-soluble ionic composition of $PM_{2.5}$ in Shanghai and Beijing, China, Atmos. Environ., 36, 4223–4234, doi:10.1016/s1352-2310(02)00342-4, 2002.

Zhang, H., Wang, S., Hao, J., Wan, L., Jiang, J., Zhang, M., Mestl, H. E. S., Alnes, L. W. H., Aunan, K., and Mellouki, A. W.: Chemical and size characterization of particles emitted from the burning of coal and wood in rural households in Guizhou, China, Atmos. Environ., 51, 94–99, doi:10.1016/j.atmosenv.2012.01.042, 2012.

Zhang, J. K., Sun, Y., Liu, Z. R., Ji, D. S., Hu, B., Liu, Q., and Wang, Y. S.: Characterization of submicron aerosols during a month of serious pollution in Beijing, 2013, Atmos. Chem. Phys., 14, 2887–2903, doi:10.5194/acp-14-2887-2014, 2014.

Zhang, M., Wang, X., Chen, J., Cheng, T., Wang, T., Yang, X., Gong, Y., Geng, F., and Chen, C.: Physical characterization of aerosol particles during the Chinese New Year's firework events, Atmos. Environ., 44, 5191–5198, doi:10.1016/j.atmosenv.2010.08.048, 2010.

Zhang, Q., Jimenez, J., Canagaratna, M., Ulbrich, I., Ng, N., Worsnop, D., and Sun, Y.: Understanding atmospheric organic aerosols via factor analysis of aerosol mass spectrometry: a review, Anal. Bioanal. Chem., 401, 3045–3067, doi:10.1007/s00216-011-5355-y, 2011.

Zhang, R., Jing, J., Tao, J., Hsu, S.-C., Wang, G., Cao, J., Lee, C. S. L., Zhu, L., Chen, Z., Zhao, Y., and Shen, Z.: Chemical characterization and source apportionment of $PM_{2.5}$ in Beijing: seasonal perspective, Atmos. Chem. Phys., 13, 7053–7074, doi:10.5194/acp-13-7053-2013, 2013.

Zhao, S., Yu, Y., Yin, D., Liu, N., and He, J.: Ambient particulate pollution during Chinese Spring Festival in urban Lanzhou, Northwestern China, Atmos. Pollut. Res., 5, 335–343, doi:10.5094/APR.2014.039, 2014.

Zhao, X. J., Zhao, P. S., Xu, J., Meng,, W., Pu, W. W., Dong, F., He, D., and Shi, Q. F.: Analysis of a winter regional haze event and its formation mechanism in the North China Plain, Atmos. Chem. Phys., 13, 5685–5696, doi:10.5194/acp-13-5685-2013, 2013.

Zheng, M., Salmon, L. G., Schauer, J. J., Zeng, L., Kiang, C. S., Zhang, Y., and Cass, G. R.: Seasonal trends in $PM_{2.5}$ source contributions in Beijing, China, Atmos. Environ., 39, 3967–3976, doi:10.1016/j.atmosenv.2005.03.036, 2005.

Zhi, G., Chen, Y., Feng, Y., Xiong, S., Li, J., Zhang, G., Sheng, G., and Fu, J.: Emission characteristics of carbonaceous particles from various residential coal-stoves in China, Environ. Sci. Technol., 42, 3310–3315, 2008.